Analysis of the Absorption and Emission Spectra of U^{3+} in $CsCdBr_3$ Single Crystal

Mirosław Karbowiak,*,† Janusz Drożdżyński,† Norman M. Edelstein,‡ and Solange Hubert§

Faculty of Chemistry, University of Wrocław, ul. F. Joliot-Curie 14, 50-383 Wrocław, Poland, Chemical Science Division, Lawrence Berkeley National Laboratory, MS 70A-1150, California 94720, and Institut de Physique Nucléaire, F-91406 Orsay Cedex, France

Received: July 29, 2003; In Final Form: October 24, 2003

Laser selective excitation and emission spectra as well as σ- and π-polarized absorption spectra have been recorded for U^{3+} ions diluted in a $CsCdBr_3$ host crystal. Three distinct U^{3+} sites were observed. For the principal site, which was attributed to a symmetric dimer center, 45 crystal-field energy levels in the 0−13250 cm^{-1} energy range were assigned. These experimentally determined levels were fitted to thirteen parameters of a semiempirical Hamiltonian representing the combined atomic, one-electron crystal field as well as two-particle correlation crystal-field (CCF) operators, with an rms deviation of 41 cm^{-1}. Above 14000 cm^{-1} strong electric-dipole allowed $5f^3-5f^26d^1$ transitions were observed. The lifetime of the $^4G_{7/2}$ fluorescing level has been measured for each of the three U^{3+} sites at liquid-helium temperatures and are 2.5, 4.3, and 7.6 μs. The emission is strongly influenced by temperature due to strong phonon coupling of the $5f^3$ states with the nearby $5f^26d^1$ states. Visible upconversion fluorescence observed when pumping the $^4I_{9/2} - (^4F_{7/2} + {}^4I_{15/2})$ absorption transitions of the principal site *A* is attributed to excited-state absorption (ESA).

1. Introduction

As host crystals for investigations of optical properties and excited-state dynamics of trivalent f-elements, single crystals of $CsCdBr_3$ have been widely employed. $CsCdBr_3$ possesses the hexagonal structure of $CsNiCl_3$, with the space group $P63/mmc(D^4_{6h})$ and two formula units per unit cell.[1] The crystal structure can be described as infinite linear chains of face sharing $(CdBr_6)^{4-}$ octahedra along the crystallographic *c* axis, with charge compensating Cs^+ ions located between the chains. Trivalent lanthanide ions are incorporated into this host predominantly as pairs replacing three adjacent Cd^{2+} ions to form dimer centers of the -$Cd^{2+}-Ln^{3+}-$(Cd vacancy)$-Ln^{3+}-Cd^{2+}$ type.[2,3] Both Ln^{3+} ions in these symmetric pairs have the C_{3v} site symmetry and are separated by approximately 6 Å. It has been estimated that at least 90% of the Ln^{3+} dopant ions take part in the formation of these centers.[2] Besides this principal site, a number of minor lanthanide sites have been also identified.

Spectroscopic investigations of actinide ions diluted in this host crystal so far have been reported only for the Cm^{3+} ion.[4] Site-selective spectroscopy was applied in order to assign the energy levels of the symmetric Cm^{3+} dimer center. The 58 levels obtained were fitted to the parameters of an empirical Hamiltonian with an rms deviation of 27.3 cm^{-1}. Weak blue upconversion was also observed when selected absorption transitions of the principal site were excited.

In recent years, crystal-field analyses of U^{3+} ions in a number of polycrystalline compounds as well as diluted in single crystals have been reported.[5,6,7,8,9] However, only in the host crystals $LaCl_3$,[10,11] $LiYF_4$,[12] and the elpasolites Cs_2MYCl_6 (M = Li or Na)[13] were the uranium ions located at a site symmetry higher than C_{2v}. Continuing our studies of crystal-field analyses of the U^{3+} ion in halogenide crystals, we turned our attention to high-symmetry hosts. In this respect, $CsCdBr_3$ and $Cs_3Lu_2X_9$ (where X = Cl or Br) single crystals are especially interesting. In our previous paper, the results of a spectral analysis and crystal-field (CF) calculations of U^{3+}:Cs_2NaYBr_6 single crystals were presented.[14] In this host crystal, the uranium ions are at site of O_h symmetry. In a $CsCdBr_3$ single crystal, the incorporated trivalent lanthanide or actinide ions are primarily at the site of C_{3v} symmetry. Moreover, the crystal field at the impurity ion can be described as the superposition of a dominant octahedral and a weaker trigonal crystal field.[15] The C_{3v} site symmetry observed in the $Cs_3Lu_2X_9$ (X = Cl, Br) type of compounds may also be considered to have a dominant O_h symmetry crystal field but with a larger distortion due to a stronger contribution of the trigonal part of the crystal field. Thus, these compounds form a suitable series of host crystals with which a comparison of the influence of the descending site symmetry on the crystal field levels of U^{3+} ions is possible.

The results of CF analysis of U^{3+} ions doped in $Cs_3Lu_2X_9$ single crystals will be presented in one of our subsequent papers. This paper presents an analysis of (i) low-temperature polarized and unpolarized absorption spectra of U^{3+}:$CsCdBr_3$ single crystals in the 3900−28000 cm^{-1} range, (ii) laser site-selective emission and excitation spectra of the crystal in the visible region at 4.2 K, (iii) the decay times of emission observed for U^{3+} ions at different sites, and (iv) the temperature dependence of the lifetime of the $^4G_{7/2}$ emitting level. Visible anti-Stokes emissions were observed after excitation of the U^{3+} energy levels located in the infrared region. 45 experimental energy levels were determined and fitted to parameters of a semiempirical Hamiltonian employing "free-ion", one-electron crystal-field, and two-particle correlation crystal-field (CCF) operators. The results are compared with those obtained for the isoelectronic Nd^{3+} ions in the same host and U^{3+} ions in various other host crystals.

2. Experimental Section

U^{3+}-doped $CsCdBr_3$ single crystals were grown by the Bridgman-Stockbarger method, using UBr_3 as the dopant. UBr_3

* To whom correspondence should be addressed. Phone: +48 71 3757304. Fax: +48 3282348. E-mail: karb@wchuwr.chem.uni.wroc.pl.
† University of Wrocław.
‡ Lawrence Berkeley National Laboratory.
§ Institute de Physique Nucléaire.

10.1021/jp036209r CCC: $27.50
Published on Web 12/06/2003

was obtained by thermal decomposition of $(NH_4)_2UBr_5 \cdot 2CH_3CN \cdot 5H_2O$ according to the procedure reported in ref 16. The uranium concentration in the starting material was 0.2 mol %. In the final sample, it may be somewhat lower due to an uneven distribution during the crystal growth. Crystals of approximately 6 mm in diameter and 2 mm in length were cleaved from the bulk and polished with fine CeO_2 powder under dry paraffin oil. All spectroscopic measurements were performed at liquid-helium temperatures using an Oxford Instruments CF-1204 optical cryostat.

Polarized absorption spectra were recorded on Cary-50 UV−vis−NIR spectrophotometer in the 3800−28000 cm^1 range with a linear polarizer oriented parallel or perpendicular to the crystallographic *c* axis. Laser-selective excitation and fluorescence spectra were recorded using a Spectra Physics model PDL-3 dye laser pumped by the second, or third-harmonic output of a Spectra Physics model GCR-3 Nd:YAG laser. Fluorescence was analyzed using a Spex model 1403 double-grating monochromator and detected by a thermoelectrically cooled Hamamatsu R943−02 photomultiplier tube. The signal was amplified by a Stanford Research model SR445 preamplifier and measured using a Stanford Research model SR250 time gated integrator. Fluorescence transients were recorded using the LeCroy model 9360 digital storage osciloscope and fitted to single or double exponential functions to obtain the fluorescence lifetimes.

3. Theory

For the energy level calculations, we have applied the effective operator model.[17,18] The observed energy levels were fitted to the phenomenological Hamiltonian $\hat{H} = \hat{H}_{FI} + \hat{H}_{CF} + \hat{H}_{CCF}$ by a simultaneous diagonalization of the free-ion Hamiltonian ($\hat{H}_{FI}$) and crystal field Hamiltonian ($\hat{H}_{CF}$ and $\hat{H}_{CCF}$). The free ion Hamiltonian is given by the equation

$$\hat{H}_{FI} = E_{ave} + \sum_{k=2,4,6} F^k(nf,nf)\hat{f}_k + \zeta_{5f}\hat{A}_{SO} + \alpha\hat{L}(\hat{L}+1) + \beta\hat{G}(G_2) + \gamma\hat{G}(R_7) + \sum_{i=2,3,4,6,7,8} T^i\hat{t}_i + \sum_{j=0,2,4} M^j\hat{m}_j + \sum_{k=2,4,6} P^k\hat{p}_k \quad (1)$$

where E_{ave} is the spherically symmetric one-electron part of the Hamiltonian, $F^k(nf, nf)$ and ζ_{5f} represent the radial parts of the electrostatic and spin−orbit interactions, and f_k and A_{SO} are the angular parts of these interactions, respectively. The α, β, and γ parameters are associated with the two-body correction terms, which represent the spin-independent interaction between configurations of equal parity. $G(G_2)$ and $G(R_7)$ are Casimir operators for the G_2 and R_7 groups and L is the total orbital angular momentum. The three-particle configuration interaction is expressed by T^it_i (i=2,3,4,6,7,8), where T^i are parameters and t_i are three-particle operators. The electrostatically correlated spin−orbit perturbation is represented by the P^k parameters and those of the spin−spin and spin−other-orbit relativistic corrections by the M^j parameters. The operators associated with these parameters are designated by m_j and p_k, respectively. For the different interaction mechanisms introduced in the Hamiltonian of eq 1, the angular parts can be evaluated exactly, whereas the radial parts are treated as parameters.

Each of the two equivalent M^{3+} sites in the symmetric pair center possess the C_{3v} symmetry. For this symmetry the crystal field Hamiltonian can be expressed in terms of phenomenological B_q^k crystal-field parameters and the $\hat{U}_q^k$ unit tensor operators as follows:

$$\hat{H}_{CF} = B_0^2\hat{U}_0^2 + B_0^4\hat{U}_0^4 + B_3^4(\hat{U}_3^4 - \hat{U}_{-3}^4) + B_0^6\hat{U}_0^6 + B_3^6(\hat{U}_3^6 - \hat{U}_{-3}^6) + B_6^6(\hat{U}_6^6 - \hat{U}_{-6}^6) \quad (2)$$

In this study, the unit tensor normalization was chosen for the one-particle crystal-field operators instead of the more usually applied spherical tensor normalization. The parameters in these two different normalizations are related by[19]

$$B_q^k(\text{spherical tensor}) = \langle l_f||C^{(k)}||l_f\rangle B_q^k(\text{unit tensor}) \quad (3)$$

where

$$\langle l_f||C^{(k)}||l_f\rangle = -7\begin{pmatrix} 3 & k & 3 \\ 0 & 0 & 0 \end{pmatrix}$$

The last term of the complete Hamiltonian represents the correlated two-electron crystal-field interactions. Following Reid,[20] the parametrization of these interactions may be written in Judd's notation[21] as a set of G_{iq}^k parameters

$$\hat{H}_{CCF} = \sum_{i,k,q} G_{iq}^k\,\hat{g}_{iq}^{(k)} \quad (4)$$

where k runs through the even integers from 0 to 12, i distinguishes different $\hat{g}_{iq}^{(k)}$ operators with identical k, and q is restricted by the crystal field symmetry.

Because there are 41 independent correlation crystal-field (CCF) parameters, it is not possible to include all of them in a fit with a set of 45 experimental data only. However, Li and Reid[22] in an analysis of a number of Nd^{3+} doped crystals have shown that the inclusion of only a few of them have markedly improved the fits and some problems with poorly fitted levels by the one-electron crystal-field operator H_{CF} could have been resolved. Parameters connected with the largest matrix elements for these levels have obviously the largest influence on the problematic multiplets. In the spectrum analysis performed for U^{3+}:$CsCdBr_3$ the most problematic multiplets were the $^2H_{9/2}$ and $^4F_{5/2}$ for which considerable discrepancies between the calculated and experimental splitting values were found. The order of the crystal-field energy levels also was not correctly reproduced. The largest values for the diagonal matrix elements for the $^2H_{9/2}$ and $^4F_{5/2}$ levels possess the G_{10Aq}^4 and G_{4q}^4 correlation crystal field (CCF) parameters, respectively. Because for the C_{3v} symmetry the q value is restricted to 0 and 3, only 4 CCF parameters may occur. Hence, the $\hat{H}_{CCF}$ Hamiltonian employing terms connected with those four CCF parameters is defined as

$$\hat{H}_{CCF} = \sum_{q=0,3} G_{10Aq}{}^4\hat{g}_{10Aq}^{(4)} + \sum_{q=0,3} G_{4q}{}^4\hat{g}_{4q}^{(4)} \quad (5)$$

To reduce further the number of independent parameters, one may assume an identical q dependence for the CCF and one-electron CF interaction parameters: $G_{10A3}^4 = (B_3^4/B_0^4)\cdot G_{10A0}^4$ and $G_{43}^4 = (B_3^4/B_0^4)\cdot G_{40}^4$. Hence, the Hamiltonian used in the presented calculations is given by

$$\hat{H}_{CCF} = G_{10A0}{}^4\left(\hat{g}_{10A0}^{(4)} + \frac{B_3{}^4}{B_0{}^4}\hat{g}_{10A3}^{(4)}\right) + G_{40}{}^4\left(\hat{g}_{40}^{(4)} + \frac{B_3{}^4}{B_0{}^4}\hat{g}_{43}^{(4)}\right) \quad (6)$$

In this way only two independent CCF parameters remain and were utilized in the fitting procedure.

In the energy level calculations, the complete (364 × 364) $SLJM_J$ matrix has been diagonalized. The calculations were performed by applying the f-shell empirical programs written

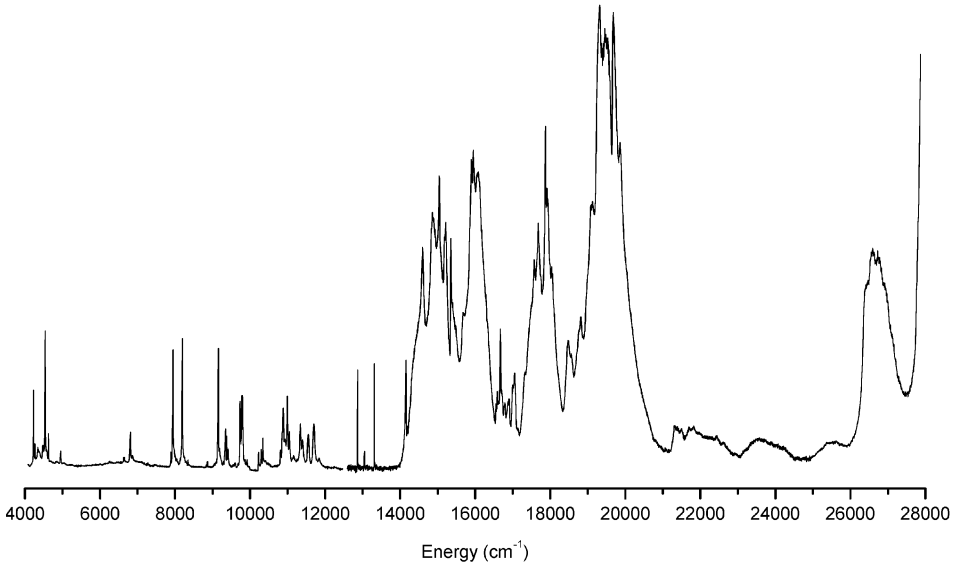

Figure 1. Unpolarized survey absorption spectrum of U^{3+}:$CsCdBr_3$ at 7 K.

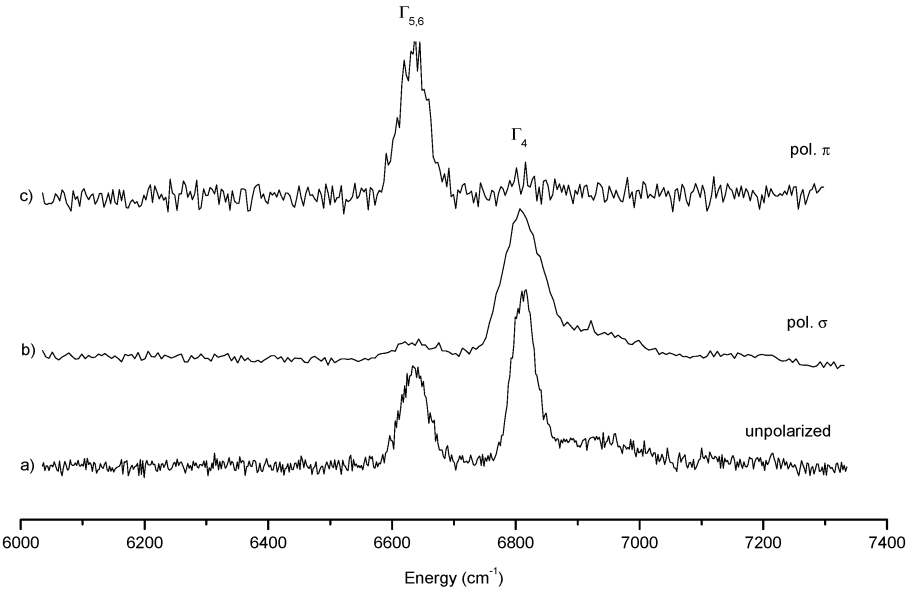

Figure 2. Unpolarized (a) and polarized (b,c) $^4I_{9/2} \rightarrow {}^4F_{3/2}$ absorption spectra of U^{3+}:$CsCdBr_3$ at 7 K. The assignment to irreducible representations is based on the polarization dependence of the crystal-field transitions.

by Reid[23] and running on a PC under the Linux Mandrake operating system. The quality of the fits to the above expressions were determined using the rms deviation (in cm^{-1}), defined as

$$\mathrm{rms} = \sum \left(\frac{(E_{\mathrm{exp}} - E_{\mathrm{calc}})^2}{(n-p)} \right)^{1/2} \tag{7}$$

where, n is equal to the number of levels and p is the number of parameters that were freely varied. To compare the magnitudes of the total crystal field strength the scalar parameter[24]

$$N_v = \left[\sum_{k,q} (B_q^k)^2 \frac{4\pi}{(2k+1)} \right]^{1/2} \tag{8}$$

has been applied.

4. Results and Discussion

4.1. Absorption Spectra. In the absorption spectra, two spectral regions may be distinguished (Figure 1). In the 4000−14000 cm^{-1} absorption range parity forbidden intraconfigurational $5f^3-5f^3$ transitions are observed exclusively. Above this range, the forbidden $5f^3-5f^3$ transitions are obscured by very intense and broad absorption bands attributed to parity-allowed $5f^3-5f^26d^1$ transitions. At an energy of about 28 000 cm^{-1}, the edge of a strong UV absorption band of the host crystals appears. The broad band observed between 26 000 and 28 000 cm^{-1} is due to $5f^2-5f^16d^1$ absorption of U^{4+} impurities.[25]

The analysis of polarized absorption spectra, measured at a sample temperature of 7 K enabled the assignment of the irreducible representations (irrep) of the observed energy levels.

In all transition regions examined in the present study, the line intensities are dominated by electric-dipole contributions.[10,26] Each of the energy levels of the $5f^3$ electronic configuration are Kramer's doublets and may be classified as having either the Γ_4 or $\Gamma_{5,6}$ symmetry in the C_{3v} double-rotation group. The electric-dipole selection rules are given for the C_{3v} symmetry in Table 1.

Figure 2 presents absorption spectra recorded in $^4I_{9/2}-{}^4F_{3/2}$ transition range. The two components of the $^4F_{3/2}$ multiplet may

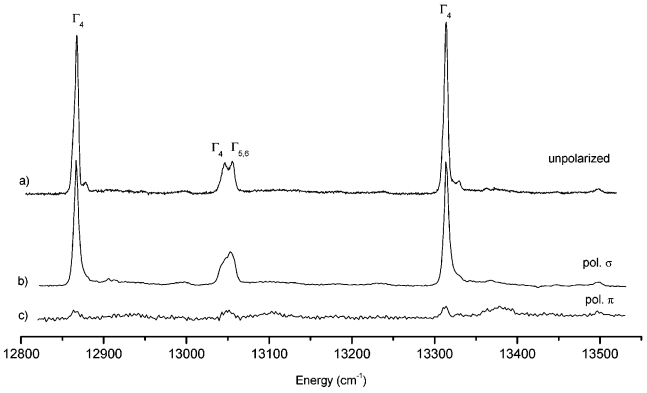

Figure 3. Unpolarized (a) and polarized (b,c) $^4I_{9/2} \rightarrow {}^4G_{7/2}$ absorption spectra of U^{3+}:$CsCdBr_3$ at 7 K.

TABLE 1: Electric Dipole Selection Rules for f^n Ions (n odd) at C_{3v} Symmetry Sites

states	Γ_4	$\Gamma_{5,6}$
Γ_4	σ, π	σ
$\Gamma_{5,6}$	σ	π

be easily distinguished. Moreover, this figure shows that in this system the polarization selection rules are operating quite effectively.

Figure 3 presents the absorption spectrum recorded in the 12 800−13 400 cm^{-1} range. The two strong lines at 12 866 and 13 312 cm^{-1} as well as a doublet with components at 13 045 and 13 052 cm^{-1} have been assigned to transitions from the ground level to the crystal-field components of the $^4G_{7/2}$ multiplet. The spectra presented in Figures 2 and 3 show that in the 0.2% U^{3+}:$CsCdBr_3$ crystal, used for absorption measurements, only one type of sites is dominant. The other sites are present at far lower concentration. The two weak lines, observed in spectrum presented in Figure 3 at the vicinity of the main lines, centered at 12 878 and 13 329 cm^{-1} are most probably due to uranium ions at other sites. The presence of U^{3+} in multiple sites is more evident in the emission spectra and will be discussed later. Further examples of absorption spectra, recorded in the $^4I_{9/2}-{}^4I_{13/2}$, $^4I_{9/2}-{}^2H2_{9/2}$, and $^4I_{9/2}-{}^4F_{5/2}$ transitions regions are shown in Figures 4, 5, and 6, respectively.

Because the emission spectra have been recorded in unpolarized light, the irrep. assignment of the Stark components of the ground level could not be directly determined. However, the symmetry of the lowest component of the ground multiplet can be deduced by a comparison of the U^{3+}:$CsCdBr_3$ absorption spectrum with those recorded for the U^{3+}- doped Cs_2NaYBr_6 and $Cs_2Lu_2Cl_9$ single crystals along with an analysis of polarized absorption transitions originating from this level. The absorption spectra for the $^4I_{9/2}-{}^4G_{7/2}$ transitions region of U^{3+} ions doped in these three hosts crystals are presented in Figure 7. As mentioned above, the U^{3+} ions in the Cs_2NaYBr_6 host are located in a pure O_h site. The C_{3v} crystal field affecting the U^{3+} ions in the $CsCdBr_3$ and $Cs_2Lu_2Cl_9$ single crystals may be described as a superposition of a dominant octahedral part and a weaker trigonal part. Under O_h symmetry, the $^4G_{7/2}$ multiplet splits into two doubly degenerate states (Γ_6 and Γ_7) and a quartet state of Γ_8 symmetry. Adding a weak trigonal (C_{3v}) distortion the Γ_6 (O_h) and Γ_7 (O_h) states become Γ_4 (C_{3v}), whereas the Γ_8(O_h) states are split into two doublets, Γ_4 (C_{3v}) and $\Gamma_{5,6}$ (C_{3v}). Hence, one should observe in the U^{3+}:$CsCdBr_3$ absorption spectrum two closely placed lines, due to transitions to levels arising from the Γ_8 cubic quartet split by the weak trigonal crystal field.

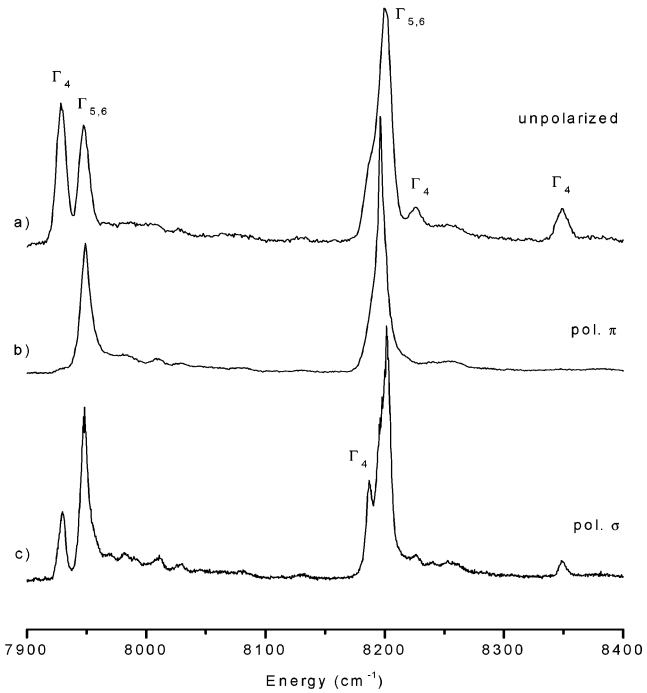

Figure 4. Unpolarized (a) and polarized (b,c) $^4I_{9/2} \rightarrow {}^4I_{13/2}$ absorption spectra of U^{3+}:$CsCdBr_3$ at 7 K.

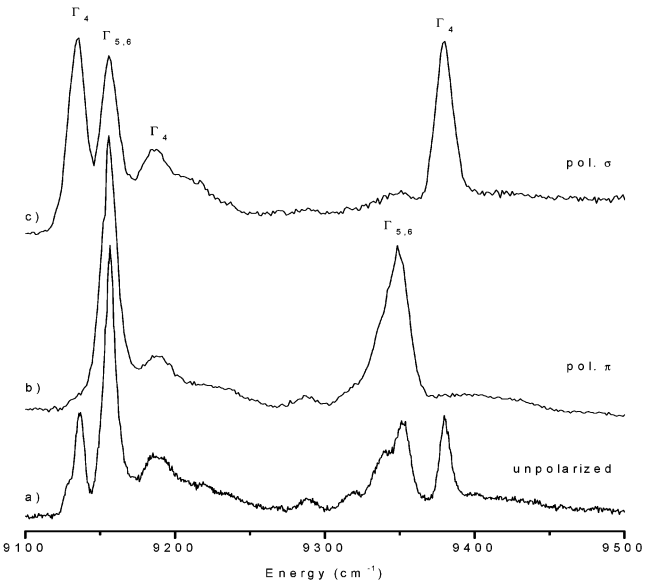

Figure 5. Unpolarized (a) and polarized (b,c) $^4I_{9/2} \rightarrow {}^2H(2)_{9/2}$ absorption spectra of U^{3+}:$CsCdBr_3$ at 7 K.

In the U^{3+}:$Cs_2Lu_2Cl_9$ host crystal, the contribution of the trigonal field is greater so a larger splitting is observed. In the absorption spectra presented in Figure 7, the level assigned as Γ_8 in the spectrum of U^{3+}:Cs_2NaYBr_6 splits into two components separated by 7 and 24 cm^{-1} for U^{3+}:$CsCdBr_3$ and U^{3+}:$Cs_2Lu_2Cl_9$, respectively. Because the Γ_6 and Γ_7 levels do not split in the lower symmetry sites, they should be assigned as Γ_4 levels in C_{3v} symmetry. In the U^{3+}:$CsCdBr_3$ spectrum, transitions to these levels are observed in σ polarization only. Thus, according to the electric-dipole selection rules, the lowest component of the ground $^4I_{9/2}$ multiplet must be assigned as $\Gamma_{5,6}$. This conclusion also has been verified by the analysis of the other observed transitions. All absorption lines assigned as transitions to the Γ_4 levels either are not observed or have considerably lower intensity in the π-polarized spectra. How-

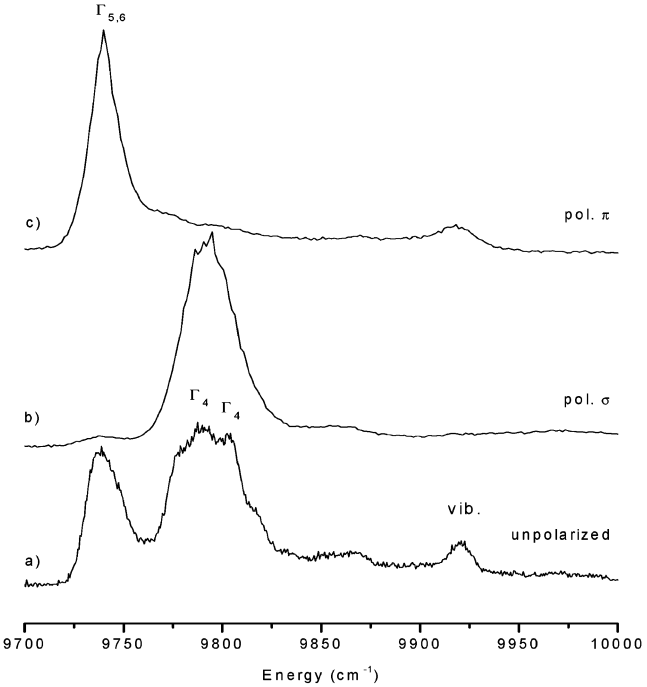

Figure 6. Unpolarized (a) and polarized (b,c) $^4I_{9/2} \rightarrow {}^4F_{5/2}$ absorption spectra of U^{3+}:$CsCdBr_3$ at 7 K.

ever, if one would assume that the ground level is of Γ_4 instead of $\Gamma_{5,6}$ symmetry, then the $\Gamma_4 \leftrightarrow \Gamma_4$ transitions should be observed both in π and σ polarization. The $\Gamma_{5,6}$ assignment of the ground level is also in accord with the ground states reported for Er^{3+} and Nd^{3+} ions doped in $CsCdBr_3$ single crystals.[27]

The analysis of the absorption spectra enabled the assignment of 40 energy levels. As mentioned earlier, the doped trivalent transition metal ions (M^{3+}) are predominantly incorporated as the symmetric $-M^{3+}-(Cd^{2+}$ vacancy$)-M^{3+}-$ dimers in the $CsCdBr_3$ single crystals. 93% of Ln^{3+} ions in Nd^{3+}:$CsCdBr_3$[28] and 95% in Tb^{3+}:$CsCdBr_3$[29] have been found to be located at this site symmetry. Because some additional lines observed in the spectrum of U^{3+}:$CsCdBr_3$ are more than 1 order of magnitude less intense, one may assume that for this system, all relatively strong absorption lines should be assigned to energy levels connected with the $-U^{3+}-(Cd^{2+}$ vacancy$)-U^{3+}-$ pairs. Henceforth this site will be referred as the major one and labeled as site *A*.

4.2. Emission and Excitation Spectra. Figure 8a presents the emission spectra recorded at 4.2 K for the $^4G_{7/2}-{}^4I_{9/2}$ transition range with excitation at 14 702 cm^{-1}. This excitation line corresponds to the broad $5f^3-5f^26d^1$ absorption transition.

The number of emission lines observed in this spectral range is inconsistent with the number of $J + 1/2 = 5$ Stark components expected for the $^4I_{9/2}$ multiplet. The energy level at 12 866 cm^{-1} has been assigned as the lowest component of the $^4G_{7/2}$ multiplet for the major site from the absorption spectrum. Thus, the emission lines observed at higher energies (12 900 and 19 217 cm^{-1}) arise from U^{3+} ions at minor symmetry sites. If it is assumed that the intensities of the emission lines reflect the concentration of each U^{3+} ion at different sites, the three most intense lines observed at 12 866, 12 825, and 12 509 cm^{-1} should be assigned to the major site (the A site) in $CsCdBr_3$. To prove this assumption and to identify the remaining lines, low-temperature site selective excitation spectra were obtained for each of the emission lines.

Figure 9 shows the excitation spectra recorded while monitoring the emission lines at 12 866, 12 900, and 12 917 cm^{-1}. The spectra presented in Figure 9 correspond to transitions from the ground level to the third and fourth Stark component of the $^4G_{7/2}$ multiplet, located in the 13 030−13 100 cm^{-1} and 13 300−13 450 cm^{-1} regions, respectively. In the excitation spectrum recorded while monitoring the 12 866 cm^{-1} emission line (Figure 9a), one observes an intense transition at 13 310 cm^{-1}. This value exactly corresponds with the energy of the fourth crystal field component of the $^4G_{7/2}$ multiplet determined from the absorption spectra, and thus proves that the emission line at 12 866 cm^{-1} as well as the absorption line at 13 310 cm^{-1} are characteristic for U^{3+} ions in the major A site. From the excitation spectra two minor sites may be identified. For the emission lines at 12 900 and 12 917 cm^{-1} the $^4I_{9/2} - {}^4G_{7/2}(4)$ absorption transitions at ∼13 340 cm^{-1} (Figure 9b) and at ∼13 365 cm^{-1} (Figure 9c) are observed, respectively. These two sites will henceforth be called as site B and C, respectively. They are not as well defined as site A, because the $^4I_{9/2} - {}^4G_{7/2}(4)$ transitions observed in the excitation spectra are split

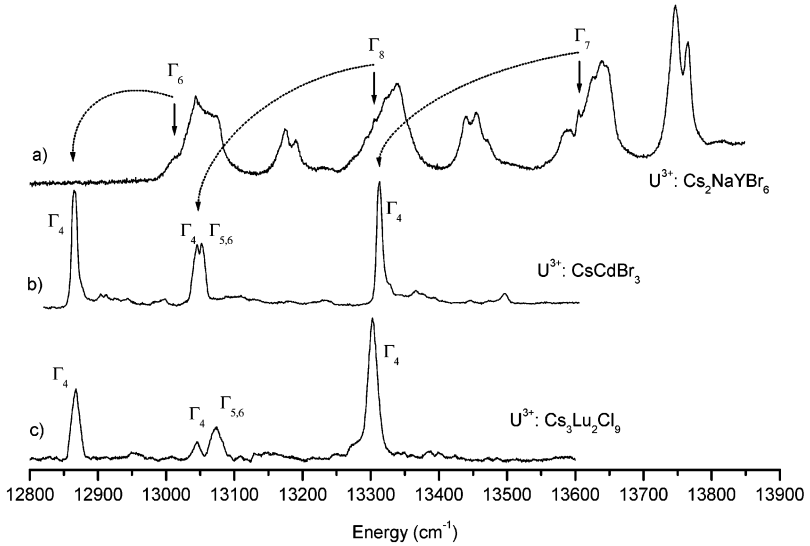

Figure 7. Absorption spectrum at 7 K showing the $^4I_{9/2} \rightarrow {}^4G_{7/2}$ transitions in the U^{3+}:Cs_2NaYBr_6 (a), U^{3+}:$CsCdBr_3$ (b), and U^{3+}:$Cs_3Lu_2Cl_9$ single crystals. The quartet state of Γ_8 symmetry splits into Γ_4 and $\Gamma_{5,6}$ doublets, when the site symmetry is lowering from O_h (Cs_2NaYBr_6) to C_{3v} ($CsCdBr_3$ and $Cs_3Lu_2Cl_9$).

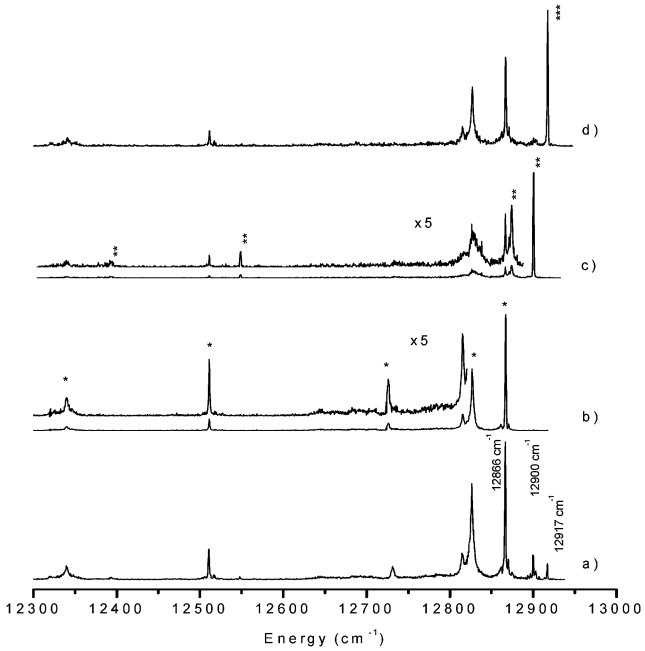

Figure 8. 4.2 K emission spectrum showing the $^4G_{7/2} \rightarrow {}^4I_{9/2}$ transitions of U^{3+}:$CsCdBr_3$, recorded after: (a) 14 702 cm^{-1} excitation, which corresponds to the broad $5f^3 \rightarrow 5f^26d^1$ transitions of U^{3+}. The emission lines observed at 12 900 and 12 917 cm^1 arise from U^{3+} ions at minor symmetry site; (b) 13310 cm^{-1} excitation, which corresponds to absorption line of U^{3+} in site A. The asterisks mark the emission lines assigned to U^{3+} ion in major site A; (c) 13 337 cm^{-1} excitation, which corresponds to absorption line of U^{3+} in site B. The double asterisks mark the emission lines assigned to U^{3+} ion in minor site B; (d) 13 369 cm^{-1} excitation, which corresponds to absorption line of U^{3+} in site C. The emission line marked with triple asterisks is due to transition between the lowest components of the $^4G_{7/2}$ and $^4I_{9/2}$ multiplets of U^{3+} in minor site C.

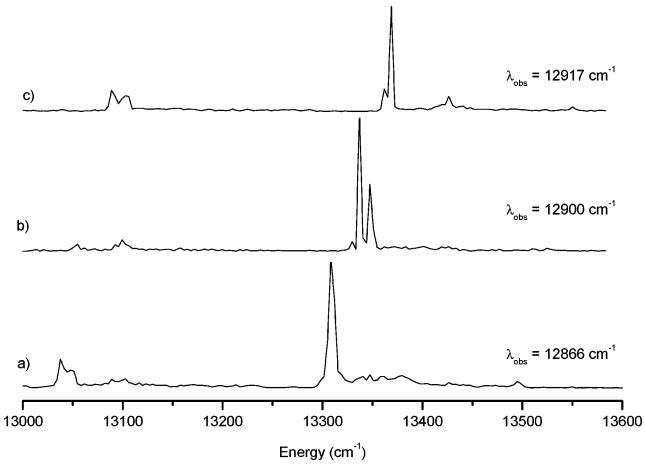

Figure 9. 4.2 K excitation spectra recorded while monitoring the emission lines at 12 866 (a), 12 900 (b), and 12 917 cm^{-1} (c) of U^{3+} ions in sites A, B, and C, respectively. The lines observed in the spectra correspond to transitions from the ground level to the third and fourth Stark component of the $^4G_{7/2}$ multiplet.

into two components observed at 13 337 and 13 348 cm^{-1} for site B and at 13 361 and 13 369 cm^{-1} for site C.

Figure 8b presents the emission spectrum recorded in the $^4G_{7/2}-{}^4I_{9/2}$ transition range with excitation energy matched to 13 310 cm^{-1} (absorption line of U^{3+} in site *A*). The lines at 12 900 and 12 917 cm^{-1}, assigned respectively to the sites B and C, disappeared.

However there are still 6 lines present instead of 5 expected. Therefore, the excitation spectra in the $^4I_{9/2}-{}^4G_{7/2}(4)$ absorption

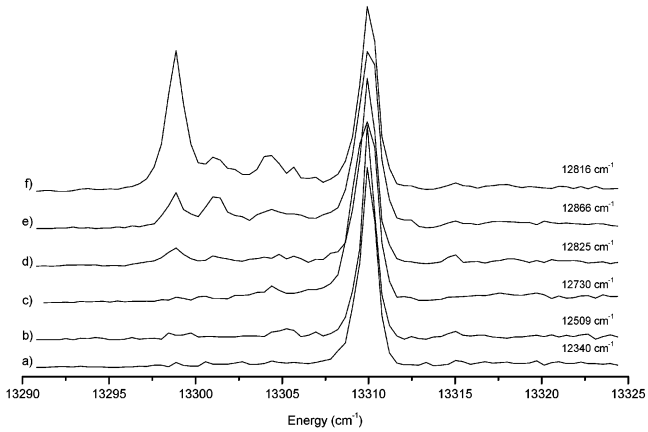

Figure 10. 4.2 K excitation spectra recorded while monitoring the six emission lines observed in spectrum shown in Figure 8b at energies of 12340 (a), 12509 (b), 12730 (c), 12825 (d), 12866 (e), and 12816 cm^{-1} (f).

range have been recorded while monitoring the 6 emission lines observed in Figure 9b. The spectra obtained are shown in Figure 10. The excitation spectra for all but one line are very similar, with the most intense absorption peak at 13 310 cm^{-1}. The spectrum observed while monitoring the 12 816 cm^{-1} emission line is markedly different, with an additional strong line at 13 299 cm^{-1} (Figure 10f).

Hence, the 12 816 cm^{-1} emission line is not considered as a characteristic for U^{3+} ions in site A. The remaining 5 lines, marked with asterisks in the emission spectrum presented in Figure 8b, have been assigned as transitions from the lowest crystal level of the $^4G_{7/2}$ multiplet to the five Stark components of the $^4I_{9/2}$ ground multiplet for U^{3+} ions in site A. On the basis of this spectrum the Stark components of the ground multiplet at energies of 0, 41, 136, 357, and 526 cm^{-1} have been determined. Because the emission spectra were recorded with unpolarized light no assignments of the irreductible representations were obtained directly from experimental data.

However, a comparison of the absorption spectra of U^{3+} ions doped in $CsCdBr_3$ and Cs_2NaYBr_6 single crystals as described earlier enabled the assignment of the lowest component as $\Gamma_{5,6}$. Under O_h symmetry, the $^4I_{9/2}$ ground multiplet splits into two Γ_8 levels and one Γ_6 level. In the Cs_2NaYBr_6 host crystal, the order of these levels is Γ_8 (0 cm^{-1}), Γ_6 (117 cm^{-1}) and Γ_8 (506 cm^{-1}). In C_{3v} symmetry, the degenerate quartet $\Gamma_8(O_h)$ splits into $\Gamma_4(C_{3v})$ and $\Gamma_{5,6}(C_{3v})$ components. Thus, the two closely spaced levels observed for U^{3+}:$CsCdBr_3$ at 0 and 41 cm^{-1} originate from the $\Gamma_8(O_h)$ level split by the trigonal crystal-field. Because the lowest Stark component has been assigned as $\Gamma_{5,6}$, the level at 41 cm^{-1} must be assigned as Γ_4. The next level, observed at 136 cm^{-1} corresponds to Γ_6 in O_h symmetry and therefore is assigned as Γ_4. The next two levels located at 357 and 526 cm^{-1} should arise from a Γ_8 cubic quadruplet and have to be assigned as Γ_4 and $\Gamma_{5,6}$. In this case however, it is not possible to choose between the two possible assignments on the basis of the experimental data. Thus, these two levels were assigned on the basis of crystal-field calculations.

Figure 8c presents the emission spectrum obtained with excitation of the 13 337 cm^{-1} absorption line, related to site B. The spectrum is dominated by an intense line at 12 900 cm^{-1} that corresponds to the transition from the lowest level of the $^4G_{7/2}$ multiplet to the lowest Stark component of the $^4I_{9/2}$ state. This line as well as the weaker lines assigned as transitions to other CF levels of the $^4I_{9/2}$ multiplet of U^{3+} ions in site B are marked with double asterisks in Figure 8c. The Stark compo-

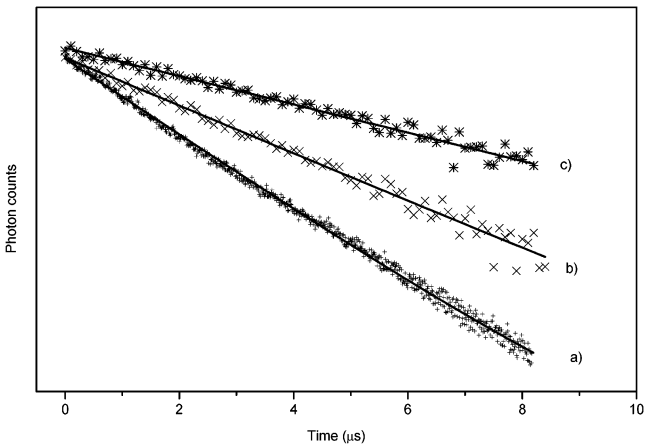

Figure 11. Fluorescence transients in a semilogarithmic scale observed for the $^4G_{7/2} \rightarrow {}^4I_{9/2}$ emission transitions of U^{3+} ions in site A (λ_{obs} = 12 666 cm^{-1}) (a), site B (λ_{obs} = 12 900 cm^{-1}) (b), and site C (λ_{obs} = 12 917 cm^{-1}) (c).

nents of the ground state of the U^{3+} ions in site B have been determined at energies of 0, 26, 351, and 507 cm^{-1}. Figure 8d presents the emission spectrum recorded while exciting with energy of 13 369 cm^{-1}, which corresponds to the absorption line of site C. The presence of the third site is shown by the intense line observed at 12 917 cm^{-1} (marked with triple asterisks), which corresponds to transitions between the lowest components of the $^4G_{7/2}$ and $^4I_{9/2}$ multiplets. However, transitions to the higher components of the ground state have not been clearly observed in the spectrum. Furthermore, some relatively strong emission lines assigned to site A were still detected.

In previous spectroscopic studies of $CsCdBr_3$ single crystals doped with rare earths ions the presence of asymmetric dimer centers of the $-Cd^{2+}-Ln^{3+}-Ln^{3+}-$Vacancy $Cd^{2+}-$ type,[30] have been reported. It has been suggested also that the energy level structure of the Ln^{3+} ions next to the Cd^{2+} ions is close to that of symmetric $-Ln^{3+}-Cd^{2+}$ vacancy$-Ln^{3+}-$ dimers (the main site A). Thus, it seems to be probable that the site symmetry assigned in this study as site B corresponds to such an asymmetric dimer. However, in this host crystal, the existence of isolated ion centers is also possible. For an accurate determination of the minor sites some further detailed studies with different concentrations of U^{3+} ions would be required. The main conclusion which results from the selective excitation and fluorescence spectroscopic studies presented here is the presence of one major and two minor symmetry sites of the U^{3+} ions diluted in $CsCdBr_3$ single crystals. The results are similar to those obtained for rare earth ions such as Er^{3+} (ref 31), Ho^{3+} (ref 32), or Pr^{3+} (ref 29) as well as Cm^{3+} (ref 4) doped in this host crystal. One may state also that the energy levels of the major site A have been unambiguously separated and assigned.

4.3. Dynamics and Upconversion. For all lines observed in the emission spectra, the decay times have been measured. Each of the recorded transients could be fit with a single-exponential decay function. The decay times recorded for lines assigned to site A (Figure 11a) are in the 2.5−2.8 μs range. This observation supports the conclusion that they are characteristic for U^{3+} ions at only one site. A very similar lifetime of 2.7 μs was obtained for the line observed at 12 816 cm^{-1}, but the excitation spectrum for this emission line was different to that obtained for the lines assigned to site A; see Figure 10. However, a similar lifetime as well as the appearance of this line in all spectra recorded while exciting U^{3+} ions in the major site A suggests that the line at 12 816 cm^{-1} is characteristic for U^{3+} in a center very

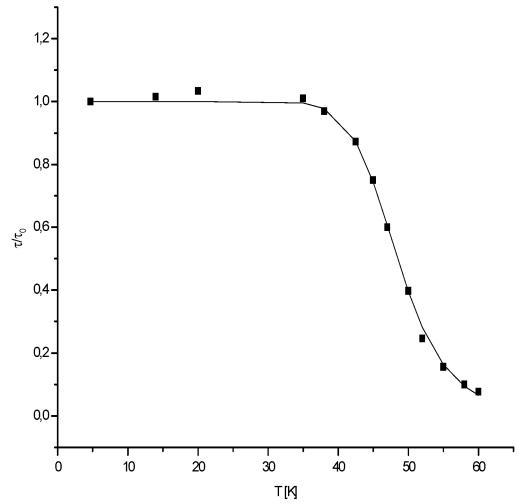

Figure 12. Temperature dependence of the $^4G_{7/2} \rightarrow {}^4I_{9/2}$ emission decay time, expressed as τ/τ_0, where τ_0 is the lifetime at 4.7 K. The curve is obtained by fitting the experimental points of eq 8.

similar to site A. The transients recorded for the U^{3+} ions in site B and C are presented in Figure 11, parts b and c, respectively.

The observed decay times are equal to 4.3 and 7.6 μs for U^{3+} ions in site B and site C, respectively, and are considerably longer than for site A.

The fluorescence lifetime measured for the $^4G_{7/2}$ level of U^{3+} in $CsCdBr_3$ is much shorter than that for the same level in Cs_2NaYBr_6 (96μs).[33] In Cs_2NaYBr_6, the U^{3+} ions experience a stronger crystal-field as compared with that in $CsCdBr_3$, but the U^{3+} ions are at a site of O_h symmetry, so only weak magnetic dipole transitions are allowed between the 5f states and a longer excited-state lifetime is observed. For the U^{3+}:$CsCdBr_3$ single crystals, the emission lifetime as well as the emission intensity strongly decrease with increasing temperature. Above $T \sim 60$ K the emission is very weak. Figure 12 presents the temperature dependence of the U^{3+} lifetime, expressed as τ/τ_0, where τ_0 is the lifetime at low temperatures. We assume that the most important factor responsible for the quenching of the U^{3+} luminescence is the proximity of the $5f^26d^1$ levels. This problem has been discussed in more detail by Karbowiak et al.[34] The observed quenching of the emission from the $^4G_{7/2}$ multiplet is caused by thermally promoted transitions to the nearby (at a distance of ~1200 cm^{-1}) $5f^26d^1$states followed by nonradiative transitions to lower $5f^3$ states.

Thus, to describe the temperature dependence of the decay times, one should use an equation that takes into consideration the activation energy. In that case, the quenching can be described by the equation

$$\tau/\tau_0 = \frac{W_D}{W_D + W_{fd}} \tag{9}$$

where τ_0 is the lifetime at low temperatures, W_D is the rate constant of downward transitions, and W_{fd} is the rate constant for upward transitions to the $5f^26d^1$ levels. If one assumes that the variation of the probability of a multiphonon process over the temperature range of the measurements can be neglected, then $W_D = 1/\tau_0$. The W_{fd} rate constant can be expressed[35] as $W_{fd} = A \exp(-E_a/kT)$, where E_a is the activation energy and A, in this case, can be treated as the decay rate constant at $T \rightarrow \infty$.

The fit of the temperature dependence of the lifetime to eq 9 with $\tau_0 = 2.54$ μs gives $A = 3.8 \times 10^{11}$ ($\pm 1.8 \times 10^{11}$) s^{-1} and $E_a = 464(\pm 31)$ cm^{-1}. If one applies for the luminescence center

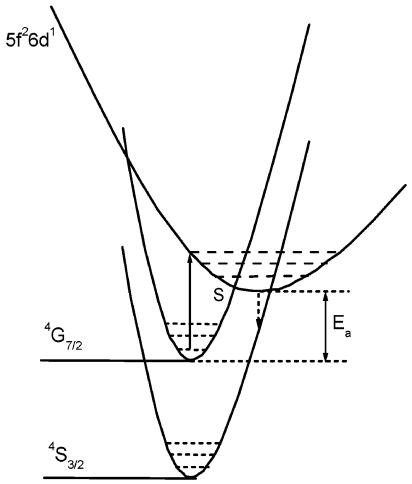

Figure 13. Single configurational coordinate model for the U^{3+} $5f^3$ and $5f^26d^1$ states explaining the temperature emission quenching (only states involved in the discussed process are shown). Electrons from the $^4G_{7/2}$ are thermally promoted to the $5f^26d^1$ state, and then relax nonradiatively to the $^4S_{3/2}$ levels. E_a is the activation energy.

a configurational-coordinate diagram (Figure 13), the activation energy will be the difference between the lowest vibrational level of the $^4G_{7/2}$ emitting state and the intersection S of the parabola of the emitting level with the curve of the lowest $5f^2$-$6d^1$ state.

Excitation with an energy of 11 547 cm^{-1}, which corresponds to the $^4I_{9/2}-(^4F_{7/2} + {}^4I_{15/2})$ absorption line of site A, resulted in anti-Stokes emission from the $^4G_{7/2}$ multiplet. The upconversion emission spectrum is very similar to a Stokes fluorescence spectrum. Only slightly different relative line intensities were observed. The excitation spectrum of the upconversion emission also coincides with the excitation spectrum obtained while monitoring the Stokes fluorescence. No rise time in the transient recorded for anti-Stokes emission has been observed. The transient could be fit to a single-exponential function, and the measured decay time of 2.8 μs is the same as that obtained for the Stokes fluorescence. Power dependence measurements give a slope of 2.1. All of these observations indicate unambiguously that for the anti-Stokes emission the excited-state absorption (ESA) mechanism is involved. For RE^{3+} ions doped in $CsCdBr_3$ single crystals, upconversion through an energy transfer upconversion (ETU) mechanism is usually very efficient.[32] However, an important difference between the RE^{3+} and U^{3+} ions are the positions of the strong and broad f−d bands, which for U^{3+}:$CsCdBr_3$ are observed at energy as low as 14 100 cm^{-1}. For the U^{3+} case, the first photon of 11 547 cm^{-1} energy excites the U^{3+} ions into the $(^4F_{7/2} + {}^4I_{15/2})$ levels. The second photon may be absorbed by the already excited ions of the $(^4F_{7/2} + {}^4I_{15/2})$ multiplet or by any other multiplet located between the $(^4F_{7/2} + {}^4I_{15/2})$ and $^4F_{3/2}$ levels that has been populated by fast multiphonon relaxation. Because parity allowed f−d transition are involved in this process the absorption of the second photon is very probable. Moreover, due to the broad nature of the f−d bands the second step is resonant in a wide range of excitation energies.

4.4. Energy Levels. From the analysis of the absorption and emission spectra of U^{3+} ions in site A, 45 energy levels were determined. The energy range available for the analysis was limited to 0−14 000 cm^{-1}, which spans the 11 lowest-energy [SL]J multiplet manifolds of the $5f^3(U^{3+})$ electronic configuration. Above this energy range, the f−f transitions could not be identified because of strong interference by the f−d bands.

TABLE 2: Calculated and Experimental Energy Levels of U^{3+} in $CsCdBr_3$

		energy (cm^{-1})				
			CF[a]		CCF[b]	
multiplet	irrep	expt.	calc.[c]	E−C	calc.[c]	E−C
$^4I_{9/2}$	$\Gamma_{5,6}$	0	21*	−21	−1	1
	Γ_4	41	15*	26	4	37
	Γ_4	136	175	−39	133	3
	Γ_4	357	360	−3	392	−35
	$\Gamma_{5,6}$	526	464	62	529	−3
$^4I_{11/2}$	Γ_4	4270	4266	4	4249	21
	$\Gamma_{5,6}$	4288	4291	−3	4274	15
	Γ_4	4340	4326	14	4317	23
	Γ_4	4517	4534	−17	4537	−20
	$\Gamma_{5,6}$	4531	4559	−28	4571	−40
	Γ_4	4629	4645	−16	4659	−30
$^4F_{3/2}$	$\Gamma_{5,6}$	6635	6691	−56	6669	−34
	Γ_4	6813	6781	32	6780	33
$^4I_{13/2}$	Γ_4	7930	7896	34	7888	42
	$\Gamma_{5,6}$	7948	7912	36	7897	51
	Γ_4		7914		7902	
	Γ_4	8186	8174	12	8160	26
	$\Gamma_{5,6}$	8194	8210	−16	8204	−10
	Γ_4	8227	8275	−48	827	−47
	Γ_4	8348	8366	−18	8363	−15
$^2H_{9/2}$	Γ_4	9134	9192*	−58	9119	15
	$\Gamma_{5,6}$	9156	9046*	109	9174	−18
	Γ_4	9180	9224	−44	926	−36
	$\Gamma_{5,6}$	9348	9379	−31	9350	−2
	Γ_4	9379	9385	−6	9361	19
$^4F_{5/2}$	$\Gamma_{5,6}$	9741	9764*	−23	9763*	−23
	Γ_4	9790	9716*	74	9687*	103
	Γ_4	9820	9756*	46	9796	6
$^4S_{3/2}$ +	Γ_4	10340	10386	−46	10385	−45
$^4G_{5/2}$ +	Γ_4	10855	10868*	−14	10907*	−53
$^4I_{15/2}$ +	$\Gamma_{5,6}$	10889	10796*	93	10845*	43
$^4F_{7/2}$	Γ_4	10931	10988	−57	10986	−55
	Γ_4	10992	11022	−30	11044	−52
	$\Gamma_{5,6}$	11053	11055	−2	11058	−5
	$\Gamma_{5,6}$	11130	11195	−65	11157	−27
	Γ_4	11250	11204	47	11234	15
	Γ_4	11342	11268	73	11284	58
	Γ_4	11404	11400	4	11403	1
	$\Gamma_{5,6}$		11475		11488	
	$\Gamma_{5,6}$	11547	11571*	4	11563*	−16
	Γ_4	11565	11561*	−24	11544*	21
	Γ_4		11597		11623	
	Γ_4	11709	11679	30	11670	39
	Γ_4		11748		11778	
	$\Gamma_{5,6}$	11842	11840	2	11842	−16
$^4G_{7/2}$	Γ_4	12866	12910	−44	12878	−12
	Γ_4	13045	13062	−17	13057	−12
	$\Gamma_{5,6}$	13052	13104	−52	13073	−22
	Γ_4	13310	13234	76	13255	57

[a] One-electron crystal-field analysis (CF). [b] Two-particle correlation crystal-field analysis (CCF). [c] Calculated Stark components denoted by an asterisk have been reordered to correspond to the experimental assignment.

These experimental energy levels were fitted to the parameters of a phenomenological Hamiltonian (eqs 1−7). The "free-ion" parameters obtained for U^{3+}:$LaCl_3$ (ref 10) as well as the twice the values of the crystal-field parameters obtained for Nd^{3+}:$CsCdBr_3$ (ref 27) have been applied as starting points in the fitting procedure. The Slater (F^k) and spin−orbit coupling parameters (ζ_{5f}) as well as six CF and two CCF crystal field parameters were allowed to freely vary. The remaining "free-ion" parameters were always fixed at their starting values. The experimental and calculated energy level values are listed in Table 2, and the best set of the parameters derived by this procedure is given in Table 3.

TABLE 3: Hamiltonian Parameters Obtained from Crystal-Field (CF) and Correlation-Crystal-Field (CCF) Analysis of U^{3+}:$CsCdBr_3$ (All Values in cm^{-1}, Except for *n*, Which Is a Number of Assigned Energy Levels Included in the Parametric Data Fits)

	fitted value[d]	
parameter[a]	CF	CCF
E_{AVG}	18919(49)	18907(40)
F^2	36918(135)	36639(110)
F^4	32942(142)	33534(122)
F^6	19906(177)	19587(144)
ζ	1601(16)	1600(13)
B_0^2	746(1424)	881(106)
B_0^4	−2143(127)	−1690(106)
B_3^4	2534(100)	2596(82)
B_0^6	−537(130)	−430(113)
B_3^6	−955(107)	−990(92)
B_6^6	857(106)	656(90)
G_{10A0}^4 [b]		3540(144)
G_{40}^4 [b]		1214(130)
n	45	45
σ[c]	50	41

[a] The atomic parameters of Hamiltonian (eq 1) not listed in this column, during the fitting procedure were kept at the constant values, taken from ref 10 (all values in cm^{-1}): $\alpha = 27.0$, $\beta = -830$, $\gamma = 1093$, $T^2 = 306$, $T^3 = 42$, $T^4 = 188$, $T^6 = -242$, $T^7 = 447$, $T^8 = 300$, $M^0 = 0.672$, $M^2 = 0.376$, $M^4 = 0.255$, $P^2 = 1216.0$, $P^4 = 912.0$, and $P^6 = 608.0$. [b] The ratios $G_{10A3}^4 = -1.154G_{10A0}^4$ and $G_{43}^4 = -1.154G_{40}^4$ were used. [c] rms standard deviation, defined by eq 7. [d] Numbers in parentheses indicate errors in determination of the parameter values.

When only atomic (H_{FI}) and one-particle crystal-field (H_{CF}) Hamiltonians were used, the 45 experimental levels were fit with an rms deviation of 50 cm^{-1} for 11 parameters.

Compared with the usual results reported for actinide ions, a quite good overall correlation between the calculated and experimental energy levels was obtained.[11,13,14] However, relatively poor agreement was found for some levels with differences on the order of 100 cm^{-1}. Also the calculation gave the lowest Stark component of the $^4I_{9/2}$ ground multiplet as Γ_4, instead of $\Gamma_{5,6}$ determined from experiment. Similarly, for some other multiplets, the order of calculated values was reversed from that obtained experimentally. The calculated splitting value of the $^2H_{9/2}$ multiplet was of 114 cm^{-1} larger than the experimental result, whereas that of $^4G_{7/2}$ was of 128 cm^{-1}, smaller than that found experimentally. This results suggest that the one-electron model is not sufficient for the description of the energy levels structure of the $5f^3$ configuration at a relatively strong crystal-field of high symmetry. A similar reordering of the two lowest components of the ground $^4I_{9/2}$ state as well as a disagreement between the calculated and experimental energy values has been observed for Nd^{3+}:$CsCdBr_3$ (ref 27). In that case, the inclusion in the calculation of the correlation crystal field interactions has noticeably decreased the discrepancies. For the U^{3+} ions in the $CsCdBr_3$ single crystal, a similar procedure has been applied (see Table 3, column 3). With the inclusion of two CCF parameters, the rms standard deviation decreased to 41 cm^{-1}, and in some cases also the wrong irrep. ordering of the crystal field levels could be corrected (Table 2, columns 6 and 7). The new values of the calculated splitting of the $^2H_{9/2}$ multiplet agree now exactly with the experimental value, and an improvement between the calculated and experimental values for the $^4G_{7/2}$ multiplet is also found, although the calculated splitting is still off by 73 cm^{-1}.

Due to the larger polarizability of the bromide ions as compared with that of the chloride ligands, the covalency of the U−Br bonds is also larger. Thus, a decrease in the electron repulsion as well as of the effective orbital angular momentum may be expected. In accord with this expectation the empirical values obtained for the F^2 and F^6 Slater integrals and ζ_{5f} spin−orbit coupling are smaller than those found for the U^{3+}:$LaCl_3$ single crystals. However, contrary to expectation, the value of the F^4 parameter is of about 9% larger than that obtained for U^{3+} in the chloride host crystal. In the fitting procedure, the values of the two-particle configuration interaction parameters cannot be properly determined for U^{3+} in $CsCdBr_3$ because they possess the largest matrix elements for multiplets positioned at high energies, and are not observed in the absorption spectra. The same holds true for the remaining minor atomic parameters which were kept at constant values in the fitting procedures, and were determined either by ab initio methods or by use of the values obtained for the U^{3+} ion in the $LaCl_3$ host. Because the operators corresponding to the α, β, γ, and F^k parameters are not orthogonal, changes in the former result in changes in the F^k parameters. Hence, the uncertainties of the determined values of two-particle configuration interaction parameters (and other minor atomic interactions parameters) appear to be compensated by the values of the F^k parameters.

In this system, similar to the results obtained for Ln^{3+} ions, the fourth-rank crystal-field parameters dominate. The absolute values of the one-electron B_q^k parameters for the U^{3+}:$CsCdBr_3$ single crystals are 1.5 (for B_0^6) to 3.2 (for B_0^2) times larger than those of Nd^{3+} in $CsCdBr_3$. The largest difference was observed for the B_0^2 parameter. This may be attributed to covalency effects for which the second-rank parameters are mostly affected. Because the spatial extent of the 5f orbitals is larger than that of the 4f it leads to the stronger CF and the larger values of all B_q^k parameters. However, because of a larger overlapping of the uranium orbitals with those of the ligands, the covalency of the U−Br bonds is larger as compared with that of the Nd−Br bonds and is reflected by a considerably larger value of the B_0^2 parameter.

With the exception of B_6^6, all other parameters possess the same signs as those reported for Nd^{3+}:$CsCdBr_3$. Because B_6^6 is largely determined by the matrix elements for $^4I_{15/2}$, this parameter is very sensitive to the assignments of the crystal-field levels within this multiplet. Transitions to this multiplet are observed in 10 800−11 900 range of the absorption spectrum, where they overlap with transitions to the $^4S_{3/2}$, $^4G_{5/2}$, and $^4F_{7/2}$ multiplets and cannot be unambiguously assigned. These problems may account for the difficulties in the determination of the value of the B_6^6 parameter. For the same reason, the values of the remaining sixth order parameters also may have been determined with somewhat lower accuracy as compared with those of second- and fourth-rank.

For O_h crystal field symmetry, the B_0^2 parameter is zero and the B_q^k/B_0^k ratios are fixed. From the above discussion, the fourth order CF parameters from this analysis should be determined with a greater accuracy than those of the sixth order, so a comparison of the B_3^4/B_0^4 ratio is of interest. In the case of O_h symmetry, the value of this ratio should be $-(10/7)^{1/2} = -1.195$. For U^{3+}:$CsCdBr_3$, this ratio is equal to -1.54 and is larger than that determined for Nd^{3+} or Er^{3+} ions in this host crystal (-1.29 for both ions).[27] The larger ratio, as well as the higher value of the B_0^2 parameter, indicates that the trigonal distortion of the CF has a more pronounced effect for U^{3+}:$CsCdBr_3$ than for the lanthanide ions. However, the energy level structure is determined by the cubic part of the CF for the most part in view of the fact that the energy level sequence within a given multiplet corresponds to that observed for U^{3+} ions in

elpasolite crystals. The effect of the trigonal part is observed as a splitting of the quartet $\Gamma_8(O_h)$ levels into two doublets of Γ_4 and $\Gamma_{5,6}$ symmetry. Because the energy difference between the Γ_4 and $\Gamma_{5,6}$ levels is relatively small as compared with the total splitting of the multiplets in O_h symmetry, one does not expect to observe a large mixing of the neighboring CF levels of the proper C_{3v} symmetry originating from the Γ_6 and Γ_7 levels of O_h symmetry.

Because of a different normalization, the B_q^k parameters must be multiplied by $(24)^{1/2}$ in order to attain a semiquantitative comparison between the B_q^k and G_{iq}^k parameters on a physically meaningful absolute scale. The obtained $|G_{10A}^4/B^4|$ ratio for the U^{3+} ions is equal to 0.43 and is considerably larger than the same ratio for Nd^{3+} ions which amounts to $\sim$0.11.[27] The correlation effects are expected to be of more importance for 5f than for 4f electrons and this may be reflected by a higher $|G_{10A}^4/B^4|$ ratio. On the other hand, the inclusion of CCF terms into the crystal-field Hamiltonian has a noticeable influence on the values of the one-electron B_q^k parameters. Thus, it seems possible that the observed improvement of the adjustment of some of the CF levels as well as that of the overall fit may not be directly related to the inclusion of CCF interactions but results from the deficiency of the applied theoretical one-electron model for description of the CF energy levels of the $5f^3$ configuration. The rms error obtained without the inclusion of CCF parameters (50 cm^{-1}) was in the range obtained for U^{3+}:elpasolite systems, where the U^{3+} ions substitute for Ln^{3+} in the O_h symmetry site (57, 61, and 43 cm^{-1} for 28, 27, and 25 energy levels of U^{3+}:Cs_2LiYCl_6, U^{3+}:Cs_2NaYCl_6, and U^{3+}:Cs_2NaYBr_6, respectively)[13,14] but is somewhat larger as compared with those reported for U^{3+} ions doped into single crystals of a lower site symmetry of the central ion.[5,9] For Nd^{3+} ions in $CsCdBr_3$, 76 energy levels were fitted to parameters of an one-electron crystal-field interaction Hamiltonian with rms = 25.8 cm^{-1} (ref 27). For Cm^{3+} ions in $CsCdBr_3$, 58 energy levels were fitted to the parameters of one-electron Hamiltonian with a rms deviation of 27.3 cm^{-1} (ref 4). However, the relatively small rms deviation for the Cm^{3+} ions may result from the fact that the symmetries of the CF levels could not be determined from experimental measurements and consequently, the experimental levels of a given multiplet were assigned to the closest calculated ones with regards to their energies.

The scalar crystal field strength parameter, N_v, determined from the crystal field analysis is equal to 3479 cm^{-1} and is almost a factor of 2 larger than that for Nd^{3+}:$CsCdBr_3$ (1854 cm^{-1}).[27] This relation is in good correlation with the experimentally observed splitting of the $^4I_{9/2}$ ground multiplet, equal to 526 and 286 cm^{-1} for the U^{3+} and Nd^{3+} ions, respectively. The N_v value obtained for U^{3+}:$CsCdBr_3$ is also similar to that obtained for Cm^{3+}:$CsCdBr_3$ (3889 cm^{-1}).[4] A considerably larger value of the N_v parameter, equal to 5300 cm^{-1}, has been reported for the $(O_h)U^{3+}$:Cs_2NaYBr_6 single crystals.[13] The Y−Br distances in Cs_2NaYBr_6 and Cd−Br in $CsCdBr_3$ are almost identical and are equal to 276.5[36] and 277.0 ppm,[1] respectively. In the simple point-charge model, the CF strength in octahedral coordination depends on the M−L distance (R) as $1/R$.[5] Thus, one would expect only a small ($\sim$1%) difference in the crystal field strength. However, the observed difference in the N_v parameter, which for the U^{3+} ions in the O_h site is a factor of 1.5 stronger than for C_{3v} site, suggests that the site symmetry is the important factor influencing crystal field strength.

5. Summary

The results of laser selective excitation and emission spectroscopic investigations indicate the presence of one major and two minor U^{3+} sites in U^{3+}:$CsCdBr_3$ single crystals. The different decay time values, obtained for the emitting $^4G_{7/2}$ level from the three sites, support this statement. The symmetric dimer center of the type $-U^{3+}-$(Cd vacancy)$-U^{3+}-$ has been attributed as the principal *A* site. σ- and π-polarized absorption spectra were recorded at 7 K in the 3800−28 000 cm^{-1} energy range. For crystals with a relatively low concentration of U^{3+} ions (<0.2 mol %), only transitions ascribed to the site A are observed in the absorption spectra. For this site symmetry, the energies of 45 crystal field levels have been determined and assigned by irreducible representations of the C_{3v} point group. Five "free-ion" and six crystal-field parameters were fitted to this experimental data set with a rms deviation of 50 cm^{-1}. The inclusion of contributions from two-electron correlation crystal-field interaction decreased the rms standard deviation to 41 cm^{-1} and enabled in some of the multiplets the correction of an erroneous irrep ordering. A comparison of the N_v crystal field strength parameters, determined for the $(O_h)U^{3+}$:Cs_2NaYBr_6 and $(C_{3v})U^{3+}$:$CsCdBr_3$ single crystals suggests that the site symmetry is an important factor influencing the crystal field strength.

The emission observed from the $^4G_{7/2}$ multiplet is quenched at $\sim$60 K, due to the thermally promoted energy transfer to the nearby ($\sim$1200 cm^{-1}) $5f^26d^1$states, followed by nonradiative transitions to lower 5f states. Visible anti-Stokes emission was observed for U^{3+} ions in site A due to the excited-state absorption (ESA) mechanism.

Acknowledgment. This work was supported by the Polish Committee for Scientific Research within the Project No. 7TO9A080 20, which is gratefully acknowledged.

References and Notes

(1) McPherson, G. L.; McPherson, A. M.; Atwood, J. L. *J. Chem. Phys. Solids* **1980**, *41*, 495.
(2) Henling, L. M.; McPherson, G. L. *Phys. Rev. B* **1977**, *16*, 1889.
(3) Henling, L. M.; McPherson, G. L. *Phys. Rev. B* **1977**, *16*, 4756.
(4) Illemassene, M.; Edelstein, N. M.; Murdoch, K. M.; Karbowiak, M.; Cavellec, R.; Hubert, S. *J. Lumin.* **2000**, *86*, 45.
(5) Karbowiak, M.; Drożdżyński, J.; Murdoch, K. M.; Edelstein, E. M.; Hubert, S. *J. Chem. Phys.* **1997**, *106*, 3067.
(6) Karbowiak, M.; Drożdżyński, J. *J. Alloys Compd.* **2000**, *300*−*301*, 329.
(7) Karbowiak, M.; Gajek, Z.; Drożdżyński, J. *Chem. Phys.* **2000**, *261*, 301.
(8) Karbowiak, M.; Edelstein, N.; Gajek, Z.; Drożdżyński, J. *Spectrochim. Acta A* **1998**, *54*, 2035.
(9) Karbowiak, M.; Mech, A.; Gajek, Z.; Edelstein, N.; Drożdżyński, J. *New J. Chem.* **2002**, *26*, 1651.
(10) Carnall, W. T.; Crosswhite, H. M. *ANL-89/39 report*; Argonne National Laboratory: Chicago, IL, 1989.
(11) Karbowiak, M.; Sobczyk, M.; Drożdżyński, J. *J. Chem. Phys.* **2002**, *117*, 2800.
(12) Simoni, E.; Louis, M.; Gesland, J. Y.; Hubert, S. *J. Lumin.* **1995**, *65*, 153.
(13) Karbowiak, M.; Drożdżyński, J.; Hubert, S.; Simoni, E.; Stręk, W. *J. Chem. Phys.* **1998**, *108*, 10181.
(14) Karbowiak, M.; Zych, E.; Dereń, P.; Drożdżyński, J. *Chem. Phys.* **2003**, *287*, 365.
(15) Barthem, R. B.; Buisson, R.; Cone, R. L. *J. Chem. Phys.* **1989**, *91*, 627.
(16) Zych, E.; Starynowicz, P.; Lis, T.; Drożdżyński, J. *Polyhedron* **1993**, *12*, 1661.
(17) Wybourne, B. G. *Spectroscopic Properties of Rare Earths*; Interscience: New York, 1965.
(18) Carnall, W. T.; Crosswhite, H.; Crosswhite, H. M.; Hessler, J. P.; Edelstein, N. M.; Conway, J. G.; Shalimoff, G. V.; Sarup, R. *J. Chem. Phys.* **1980**, *72*, 5089.

(19) Quagliano, J. R.; Richardson, F. S.; Reid, M. F. *J. Alloys Compd.* **1992**, *180*, 131.
(20) Reid, M. F. *J. Chem. Phys.* **1987**, *87*, 2875.
(21) Judd, B. R. *J. Chem. Phys.* **1977**, *66*, 3163.
(22) Li, C. L.; Reid, M. F. *Phys. Rev. B* **1990**, *42*, 1903.
(23) Reid, M. F., University of Canterburry, New Zealand, private communication.
(24) Auzel, F.; Malta, O. L. *J. Phys. (France)* **1983**, *44*, 201.
(25) Karbowiak, M.; Drożdżyński, J. to be published.
(26) Karbowiak, M.; Drożdżyński, J. *Mol. Phys.* **2003**, *101*, 971.
(27) Quagliano, J. R.; Cockroft, N.; Gunde, K. E.; Richardson, F. S. *J. Chem. Phys.* **1996**, *105*, 9812.
(28) Barthem, R. B.; Buisson, R.; Madeore, F.; Vial, J. C.; Chaminade, J. P. *J. Phys.* **1987**, *48*, 379.
(29) Berdowski, A. M.; Lammers, M. J. J.; Blasse, G. *J. Chem. Phys.* **1985**, *83*, 476.
(30) Neukum, J.; Bodenschatz, N.; Heber, J. *Phys. Rev. B* **1994**, *50*, 3536.
(31) Goldner, Ph.; Pellé, F. *J. Lumin.* **1993**, *55*, 197.
(32) Mujaji, M.; Jones, G. D.; Syme, R. W. G. *Phys. Rev. B* **1993**, *48*, 710.
(33) Dereń, P. J.; Stręk, W.; Zych, E.; Drożdżyński, J. *Chem. Phys. Lett.* **2000**, *332*, 308.
(34) Karbowiak, M.; Mech, A.; Drożdżyński, J.; Edelstein, N. M. *Phys. Rev. B* **2003**, *67*, 195108.
(35) Mott, N. F. *Proc. R. Soc. London, Ser. A* **1938**, *167*, 384.
(36) Reber, C.; Güdel, H. U.; Meyer, G.; Schleid, T.; Daul, C. A. *Inorg. Chem.* **1989**, *28*, 3249.